RAJA S.
PRABHAT KUMAR MANDAL
P. S. PAUL
and
ARKA JYOTI DAS

Prediction of coal bump with respect to local mine stiffness and post-failure stiffness using numerical modelling

In India, coal deposits under the shallow depth of cover amenable by opencast and underground mining are fast exhausting and the focus is being shifted towards the deep-seated coal deposits. But, due to the complex geo-mining conditions, techno-economic indices and non-availability of suitable technological solutions, the mining industry is facing tremendous difficulties to exploit the deep-seated coal deposits. Deep-seated coal deposits require immediate attention for its successful exploitation. Underground exploitation of the deep-seated deposits faces a number of geotechnical problems like coal bumps, pillar squeezes, sudden collapse, floor heaving etc. Coal bump is the most difficult, hazardous, long-standing engineering problem associated with the underground coal mining nearly from past three centuries. Coal bump induces the catastrophic failure of mine structures resulting in loss of life and damage to the machinery. If anyone could identify the burst-proneness before the commencement of the mining operation, a suitable method of mining can be suggested for efficient extraction of coal and can avoid the major strata control problems. In this paper, a brief review of causes, occurrence and prediction of coal bumps has been described. A case study mine has also been considered for prediction of coal bump using numerical modelling.

1.0 Introduction

The factor of safety of a pillar is the ratio between the strength of the pillar and the applied stress. When the applied stress exceeds the strength of the pillar, the pillar is subjected to fail. In an underground mine, whenever extraction is carried out, failure of the surrounding strata/rock mass/pillar is expected. If the failure takes place in a stable and regular manner, then it can be managed. If the failure is inconsistent or abrupt in nature, then it causes severe damage to the working which results in the risk of the life of men and machinery involved in the process.

Bump or burst encountered during underground extraction is such a critical failure issue which is generally inconsistent or abrupt in nature and requires a great attention to improve strata management and control for enhanced productivity and safety of the working. It occurs generally when there is a sudden release of accumulated strain energy from the coal pillar/surrounding strata. In the case of underground coal mining, it is referred to as a coal bump or pillar bump.

Coal bump is a violent failure of a coal pillar or sudden release of stored strain energy from coal pillar or eruption of violent seismic waves due to high stress in a developing or developed underground coal mine, which expels a large amount of coal/rock into the gallery or working face (Crouch and Fairhurst, 1974; Kidybinski,1981; CMRI report, 1994; Khair, 1985; Sheorey et al.,1997b; Chase et al., 2002; Iannacchione and Stephen, 2008; Wen et al,2016).

Coal bump can be widely categorised as pressure bump or shock bump. Pressure bumps occur when the stress over a pillar exceeds the strength of the pillar resulting in violent damage. Shock bumps occur due to the failure of the adjoining roof, causing the stress redistribution on the pillar and the shock waves produced due to roof failure are transferred to pillar resulting in catastrophe. Haramy and McDonnel (1988) reported that coal bump is variedly classified based on nature of the occurrence, mine, and country. They have reported that in Poland, bumps are classified as either seam, roof, or floor bumps, depending on the area of failure and in RSA, bumps are classified as a ring, shear, or pillar bumps, depending on the stress and failure mechanisms.

The first coal bump was reported nearly three centuries

Messrs. Raja S., Ph.D. Research Scholar, Department of Mining Engineering, Indian Institute of Technology (Indian School of Mines), Dhanbad 826 004 and Assistant Professor, Department of Mining Engineering, Acharya Institute of Technology, Bengaluru 560 107, e-mail: rajas@acharya.ac.in, Prabhat Kumar Mandal, Senior Principal Scientist, e-mail: pkmandal@gmail.com / pkmandal@cimfr.nic.in and Arka Jyoti Das, Scientist, Mine Design & Simulation Section, CSIR-Central Institute of Mining and Fuel Research, Dhanbad 826 015, e-mail: arkajyoti19@gmail.com / arkajyoti@cimfr.nic.in and P. S. Paul, Assistant Professor, Department of Mining Engineering, Indian Institute of Technology (Indian School of Mines), Dhanbad 826 004, e-mail: drpspaul@gmail.com

ago in Britain in the year 1738. The major deep underground coal mining countries have suffered a lot from the coal disaster in the 19th and 20th centuries. The coal bumps are prone at a higher depth of mining, geological faults, and strata, but still, the solution to predict the coal bump is in a predicament (Dou, 2001; Pan et al., 2003; Zhang et al., 2017; Jiang et al.,2017). Chinakuri is the deepest underground coal mine in India, where mining was taking place at an early 700m depth of cover and the reserves were ranging from 600 to 1200m. However, mining of the Dishergarh coal seam has always been a problem, mainly due to the occurrence of coal bumps (Petr et al., 2010; CMPDI, 2015). Some metal mines in India are operating at more 900m of depth are Jaduguda uranium mine, Sindesar Khurd mine and Rampura Agucha mine (Anon1, 2017).There are many statistics reported worldwide regarding the occurrence of coal bump from early 1900 to the present, where the underground coal mining is more prominent in some countries like China, USA, Czech Republic, India and Germany. As stated by Ghose (1988), the earliest coal bumps known in India in the year 1920. From 1944-1986, a total of 100 bumps and the fatalities count about 141 were reported. Wen et al. (2016) have stated that there are considerably 50 deep underground coal mines and 80 deep underground metal mines working at a depth greater than 1000m worldwide. He has stated that in 2006-2013, 35 coal bumps reported and about 300 people have lost their lives and many more scenario over the worldwide were quoted by Justine et al. (2016) and Jiang et al. (2017). Brauner (1994) stated that, at a minimum distance of 10m, if there are no hard strata above the coal seam at least of 5m thick, then the seam is prone to bump.

Some of the causes of coal bump proposed by Crouch and Fairhurst (1974) are (i) manner in which the over stress is produced, physical characteristics, strength of the coal and rock being stressed, (ii) immediate source of the energy that causes the particles produced to be thrown violently from the failing mass, (iii) method of mining, (iv) kind and thickness of the bed composing overburden, (v) dimensions of the pillar, (vi) stiffness of the coal pillar and crushing strength, (vii) roof and floor characteristics (which does not heave readily) and (viii) proximity of geological disturbances. Further, it was simplified by Sheorey and Singh (1988) by considering the following: (i) considerable large thickness of overburden, (generally, more than 300m), (ii) structurally strong coal, (iii) massive, strong and stiff roof strata, (iv) competent floor not easily subjected to heaving and (v) the mining method causing development of high value of stresses. In recent years, Zhao and Jiang (2009) have proposed some of the factors affecting/influencing coal bumps are vertically stress, size of pillar during extraction, width to height ratio, depth of the coal seam, local stiffness and post-failure stiffness, energy release ratio (includes the effects of depth, coal properties and geological structures), disturbed ratio (includes mining method and blasting or earthquakes) and coal pillar stability index (includes geometry of the pillars and the surrounding rocks conditions). In many cases it will not be a single cause listed above to result in a bump; it is usually a combination of many causes leading a coal bump (Rice, 1934; Crouch and Fairhurst, 1974; Sheorey and Singh, 1988; Mark and Chase, 1997; Iannacchione and Stephen, 2008; Zhao and Jiang, 2009).

A number of detection, monitoring and predicting techniques of coal bump are available and follows as: face observation (conventional method of observing the change in working face), seismic monitoring (being used for post-event analysis), probe drilling (a small micro-excavation in the coal seam and observe the seam reaction to the same), acoustic and thermal precursors (to monitor bump proneness based on thermal infrared characteristics, stress/strain measurements and acoustic emission monitoring), microgravity method (uses rock mass deformations, changes in gravity intensity, and change in density distribution to evaluate bump-prone areas), rheological method (incorporates the rate of stress relaxation and the level of coal disintegration to predict coal bumps), rebound method (from resilience tests conducted in-situ or on core samples), convergence measurements method (convergence of roof and floor by instrumentation and monitoring), on-site detection device method (rock instrumentation), photo-elastic method (polarized light is used to view object under stress based on their interference, it is compared to applied stress intensity and direction), energy disturbance analysis (relationship between magnitude of earthquake and energy is used to predict the rock burst), electromagnetic radiation based on frictional effect, and numerical modelling (Haramy and McDonnel, 1988; Yixin et al., 2009; Wang et al., 2013; Wen et al., 2016).

Numerical modelling has been used to predict/investigate bump proneness by estimating amount of strain energy released, or by determining the local mine stiffness and comparing with the post-failure stiffness, or by large/rapid deformation of roof, or based on stress-strain analysis, or energy release ratio, (Sheorey, 1997b; Zipf, 1999; Yavuz, 2001; Hongwei et al., 2013; Garvey, 2013; Ozbay, 2015). Using the geo-mining conditions, numerical modelling can be used for scientifically predicting the impact of the identified parameters towards the post and pre-mining stresses on strata contributing to coal bumps using FLAC3D (Itasca, 2012).

The prediction of bump proneness in numerical modelling involves three stages as follows:

Stage I – Using numerical model to determine the local mine stiffness,

Stage II – Using numerical model to determine post peak failure stiffness and

Stage III – Comparing the tangent of local mine stiffness with post-peak failure characteristic curve.

Based on the analogy between laboratory test specimens and mine pillars, Salamon (1970) developed a criterion i.e. if

the local stiffness is lesser than the post-failure peak stiffness of the pillar as shown in Fig.1, then the pillar fails in an unstable manner or violently and prone to a coal bump (Zipf, 1999; Yavuz, 2001).

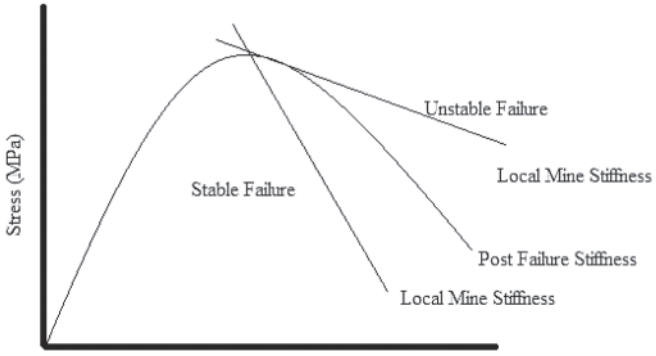

Fig.1 Stable failure or unstable failure depending upon the local mine stiffness and post-failure stiffness

2.0 Local mine stiffness

Local mine stiffness can be described as the load-deformation characteristics between hanging and footwall or roof and floor. In assessing the stability of a mining structure like pillars and to analyse the coal bump, it is generally used to determine the local mine stiffness and to compare it with the post-failure stiffness of the pillar. If the local stiffness is lesser than the post-failure peak stiffness of the pillar, it results in violent failure (Yavuz,2001).

A comparative study has been carried out based on the geo-mining conditions of Digwadih colliery of Tata Steel situated in Dhanbad district of Jharkhand. The mine is extracting coal at a depth of around 483m by bord and pillar method. This mine is considered with the observation that sometimes a little amount of coal thrown from the pillar during splitting operation, which is a sign of asudden release of energy and may be considered a near to burst-prone mine. A finite difference method like FLAC3D can be used to analyse the local mine stiffness of a pillar (Zipf, 1999; Yavuz, 2001). Two cases are considered for studying the local mine stiffness using FLAC3D i.e. 483m representing an actual depth of Digwadih colliery working and 300m for initial study and comparison. A numerical model is developed for the geo-mining conditions and the properties listed in Tables 1and 2. Some of the rock properties of the formation are taken from available tested data and non-available properties are assumed. Fig.2 shows the grid of the numerical model of underground conditions of coal seams representing the numerical models where the thickness of seam is 3.02m with pillar size 48m × 48m.

After the grid formation, the model has to be subjected to in-situ stresses (elastic model). The in-situ stresses are well-known factors that influence the stability of an underground structure.

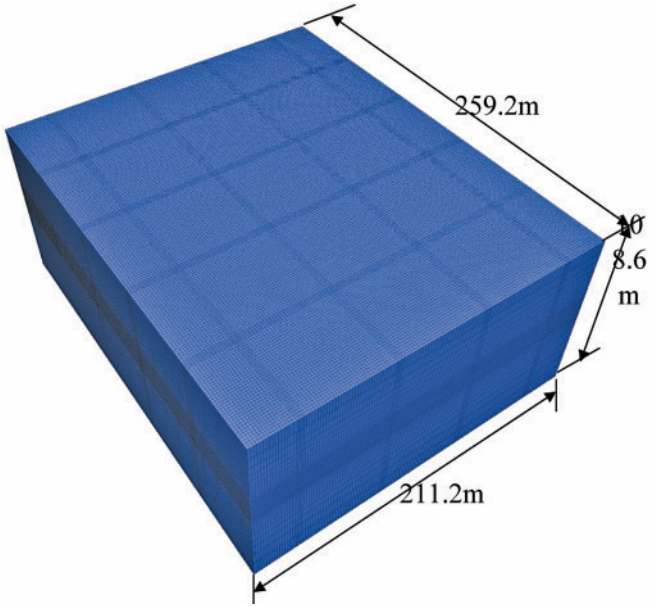

Fig.2 Numerical model grid of underground condition

TABLE 1: DIMENSIONAL DETAILS OF PILLAR FORMATION IN THE SEAM USED IN THE MODEL

Parameter	Dimension
Size of the pillar	48m × 48m (corner to corner)
Gallery width	4.8m
Development height	3.02m
Depth of cover for initial study	300m
Depth of cover for the case study mine	483m

TABLE 2: ROCK MASS PROPERTIES USED FOR DIFFERENT FORMATIONS OF BOREHOLE NO. 19 OF DIGWADIH COLLIERY

Formation*	Thickness (m)	Young's modulus (MPa)	Density (kg/m^3)	σ_c (MPa)	σ_t (MPa)	RMR
Floor	50	7.5	2578	95.7	8.84	51
Coal seam	3.02	3	1606	32.55	3.5	51
Shale	0.8	3.98	2578	60.60	4.83	44
Fgsst	0.82	4.54	2278	95.70	8.84	42
Shale	1.21	4.0	2575	70.70	7.00	37
Cgsst	13.06	6.49	2158	38.40	3.88	55
Mgsst	39.90	6.99	2378	40.00	4.40	60

*Fgsst – Fine-grainedsandstone, Cgsst – Coarse-grainedsandstone, Mgsst – Medium grained sandstone

It is, therefore, necessary to estimate the stresses as realistically as possible. Particularly, the knowledge of in-situ horizontal stress condition is an important parameter to design of an underground mining structure.

Based on a thermo-elastic shell model of the earth, Sheorey (1994) proposed an equation for the average in-seam horizontal stress. In this theory, it is observed that the mean in-situ horizontal stress (mean of the major and minor horizontal stresses) depends on the elastic constants (Young's modulus – E, Poisson's ratio – v), the coefficient of thermal expansion (β) and the geothermal gradient (G). This equation gives the value of mean horizontal stress as:

$$\sigma_h = \frac{\nu}{1-\nu}\sigma_v + \frac{\beta EG}{1-\nu}(H+1000) \text{ MPa} \quad \text{... (1)}$$

where,

H = Depth of cover in meter,

σ_v = Vertical stress and

σ_h = Horizontal stress.

In the study by Sheorey et al. (2001), this equation is shown to fit stress measurement data from different parts of the world quite well. In absence of measured data for Indian coalfields, in-situ stresses are simulated according to the Eq. (1).

The vertical in-situ stress, induced due to gravity, is taken as:

$$\sigma_v = 0.025H \text{ MPa} \quad \text{... (2)}$$

Then putting Eq. (2) and the following values as per Sheorey (2001) for Indian coal measures in Eq. (1):

v = 0.25, β = 3×10^{-5} /°C, E = 2000 MPa, G = 0.03°C/m

We obtain the mean horizontal stress as:

$$\sigma_h = 2.4+0.01H \text{ MPa} \quad \text{... (3)}$$

Although the available numbers of in-situ stress measurement data for Indian coalfields are only a few, this equation has good agreement with some measured data in India. Among these, the measurements by erstwhile CMRI (CMRI Report, 2002) are of considerable importance and it is observed that the horizontal stress field is not highly anisotropic but supports Eq. (3). Murli Mohan et al. (2001) also showed that Eq. (3) fits well during the study for estimation of pillar strength in coal mines taking failed and stable pillars case studies.

The shear strength and friction angle are estimated using Sheorey's failure criterion (Sheroey, 1997a) for rock masses which follows the 1976 version of rock mass rating (RMR) of Bieniawski (1976) for reducing the laboratory strength parameters to give the corresponding rock mass values. This criterion is defined as:

$$\sigma_1 = \sigma_{cm}\left(1+\frac{\sigma_3}{\sigma_{tm}}\right)^{b_m} \text{ MPa} \quad \text{... (4)}$$

where σ_1 and σ_3 are major and minor principal stresses at failure and the rock mass strength parameters are defined by:

$$\sigma_{cm} = \sigma_c \exp\left(\frac{RMR-100}{20}\right) \quad \text{... (5)}$$

$$\sigma_{tm} = \sigma_t \exp\left(\frac{RMR-100}{27}\right) \quad \text{... (6)}$$

$$b_m = b^{RMR/100} \quad b_m < 0.95 \quad \text{... (7)}$$

where,

σ_1 = Triaxial strength of rock mass, MPa

σ_3 = Confining stress, MPa

σ_c = Compressive strength of intact rock, MPa

σ_t = Tensile strength of intact rock, MPa

b = Exponent of intact rock which controls the curvature of triaxial curve

σ_{cm} = Compressive strength of rock mass, MPa

σ_{tm} = Tensile strength of rock mass, MPa

RMR = Bieniawski (1976) rock mass rating

b_m = Exponent for rock mass corresponding to the intact rock constant defined above.

In the above equations, the subscript m stands for the rock mass, where σ_c and σ_{cm} are the compressive strengths of intact rock and rock mass respectively. σ_t and σ_{tm} are tensile strengths of intact rock and rock mass respectively. σ_1 and σ_3 are major and minor principal stresses respectively at the time of failure b and b_m are constants.

For estimating these parameters, only the value of the compressive strength is known. Then the b = 0.5 is taken as the most representative value, as seen from a large number of test data published earlier (Sheorey, 1997a). The rock mass shear strength τ_{sm}; the coefficient, μ_{0m} and the angle of internal friction, ϕ_{0m} are obtained as:

$$\tau_{sm} = \left(\sigma_{cm}\sigma_{tm}\frac{b_m^{b_m}}{(1+b_m)^{1+b_m}}\right)^{1/2} \quad \text{... (8)}$$

$$\mu_{0m} = \frac{\tau_{sm}^2(1+b_m)^2 - \sigma_{tm}^2}{2\tau_{sm}\sigma_{tm}(1+b_m)} \quad \text{... (9)}$$

$$\phi_{0m} = \tan^{-1}(\mu_{0m}). \quad \text{... (10)}$$

It is observed that the values of shear strength, τ_{sm} and friction angle, ϕ_{0m} so determined as per Eqn. (8) and (9) needs to be adjusted slightly. There is a slight adjustment required to incorporate the fact that the Mohr-Coulomb strain softening plasticity model in FLAC3D uses the linear Mohr-Coulomb criterion, while the Sheorey criterion is non-linear (Murli Mohan et al., 2001; Mandal, 2009).

The numerical model is subjected to rock properties and in-situ stresses as listed in Tables 2 and 3. The model runs until it reaches the equilibrium. Now, using a Mohr-Coulomb

strain softening model (plastic), the development of the gallery is simulated in the model with remaining of 15 pillars (3 in the x-direction and 5 in the y-direction) with in-situ stresses used in the modelas shown in Fig.3.

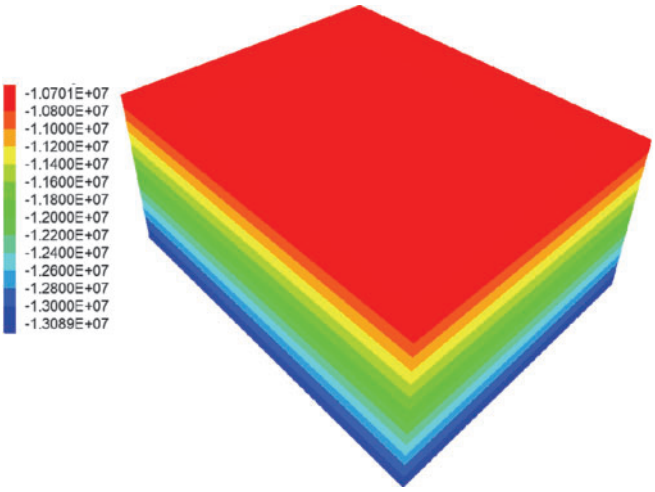

Fig.3 Development of vertical in-situ stress in the model

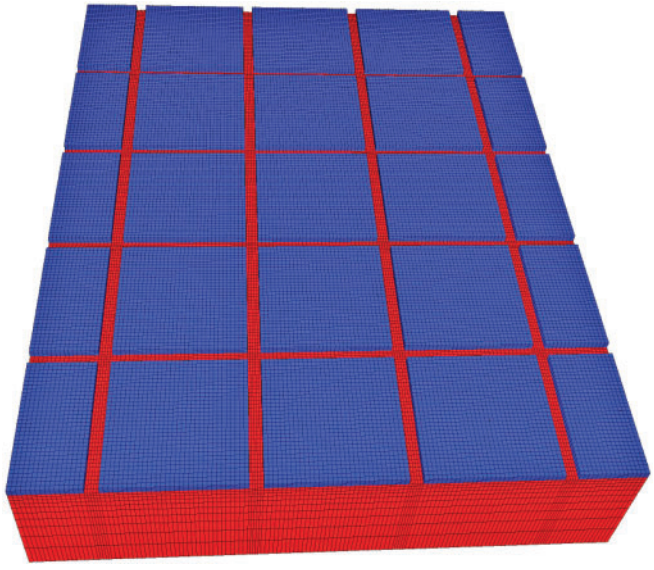

Fig.4 Numerical model of the developed coal seam

TABLE 3: IN-SITU STRESSES USED IN THE MODEL

Depth (m)	Truncated load (m)	SXX (MPa)	SYY (MPa)	SZZ (MPa)	Applied-SZZ (MPa)
300	241.98	5.4	5.4	7.50	6.03
483	424.39	7.23	7.23	12.07	10.61

Before the development of the galleries in the model, the strain softening parameters have to be obtained. The Mohr-Coulomb strain softening properties (Cohesion, friction angle and dilation angle) are determined by a single pillar test run the model (Sheorey, 1997a; Zipf, 1999; Murli Mohan et al., 2001; Mandal, 2009). Determining the Mohr-Coulomb strain softening parameter in real practice is more difficult, which is done easily by test run model.

The single pillar test run model acts as the laboratory estimation of uniaxial compressive strength using servo testing machine. It is good to run test pillar models with different sets of strain softening parameters for determination of the pillar strength matching with empirically calculated pillar strength values based on empirical pillar strength formula developed by Sheorey (1997a) which has a good agreement with the field results (Murli Mohan et. al., 2001; Mandal, 2009).

A number of test trials are carried out on the single pillar with different width and height ratios and suitable representative Mohr-Coulomb strain softening parameters are estimated as a back analysis (Heerden, 1975). By considering symmetry conditions of the pillar formation, one pillar is modelled as shown in Fig.5.

After forming the roadways in the model, the top of the model is fixed in the vertical direction and a constant velocity 10^{-5} m/s is applied. Application of zero vertical displacement at the model bottom and zero horizontal displacement at the four vertical symmetry planes are the other boundary conditions adopted in the model. 50m of the cover and 50m of the floor are modelled in the case of 300m depth of coal seam and 58.61m of the cover and 50m of the floor are modelled in the case of 483m depth of the coal seam with seam thickness of 3.02m. The width to height ratios of pillar ranging from 2 to 5 (say, widthsare equal to 6.04m, 7.55m, 10.55m, 12.08m, 15.1).

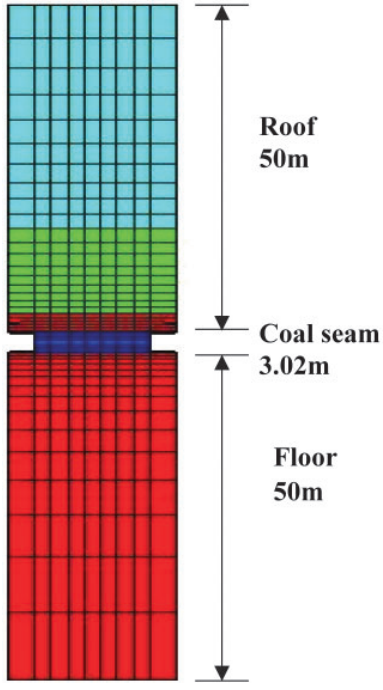

Fig.5 An example of FLAC3D grid showing a quarter pillar modelling used for determining Mohr-Coulomb strain softening parameter and post failure stiffness

The model is assigned with the strain softening parameters by trial and error until the obtained strength of the pillar is matched with the strength estimated by the Sheorey pillar strength formula as shown in Eqn.10. After declaring the model as a strain-softening model, it is allowed to run a few steps before the excavations. This process is adopted to minimize transient stress before fixing the top boundary and application of vertical load. An overall stress-strain curve for an individual pillar could be obtained using

FISH programming facility of the FLAC3D by averaging vertical stress and the vertical deformation histories across the top of the pillar. Therefore, the average vertical stresses and the average vertical strain in the pillar are continuously monitored during the model run and plotted as shown in Fig.6. The failure of the pillar is a gradual process, as observed in FLAC3D during the model run, the pillar starts failing at the outer edges and proceeds the towards the center of the core, and the horizontal stress falls little due to crushing of the pillar (Salamon, 1992; Sheorey, 1997a) as shown in Fig.7 (a to d). Sheorey pillar strength formula is written as:

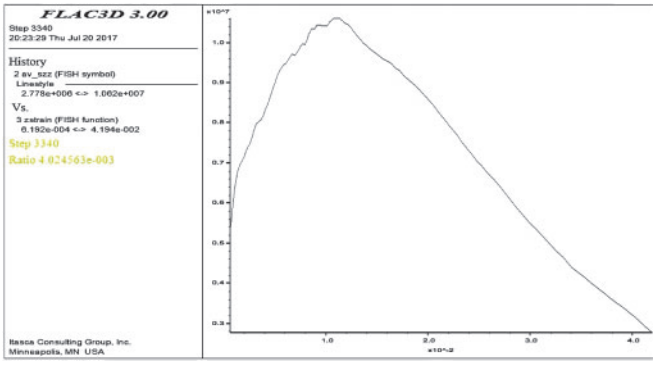

Fig.6 Average stress vs. strain curve/post failure load-convergence curve

$$S = 0.27 \times \sigma_c \times h^{-0.36} + (H/250 + 1)\,(W_e/h - 1)\ \text{MPa} \quad \ldots \quad (11)$$

where,

σ_c = Uniaxial compressive strength of coal in MPa,

h = Working height in m,

H = Depth of cover in m,

W_e = Effective pillar width = $4A/P_c$

A = Area of pillar = $L_1 \times L_2$ and

P_c = Perimeter of the pillar (corner to corner) = $2 \times (L_1 + L_2)$

Once the Mohr-Coulomb strain softening parameter determined, the same is used in the main model during the development of gallery (4.8m). After the development of the gallery, the load/average stress on the middle pillar is obtained (Mandal, 2009).

Using a FISH (an in-built programming language of FLAC3D) file the average vertical stress concentration on the pillar and the average convergence (roof and floor) is determined. Out of 15 pillars in the coal seam of the model, the middle pillar is removed as shown in Fig.8 to determine the average convergence between roof and floor.

The models give the roof-to-floor convergence C_p with the pillar in place, roof-to-floor convergence C_e with the middle pillar removed and σ_z the average vertical stress on the pillar. Then, the local mine stiffness is calculated as per Eqn. 12:

$$\kappa = \frac{\sigma_z A}{C_e - C_p} \quad \ldots \quad (12)$$

where A is the plan area of the pillar.

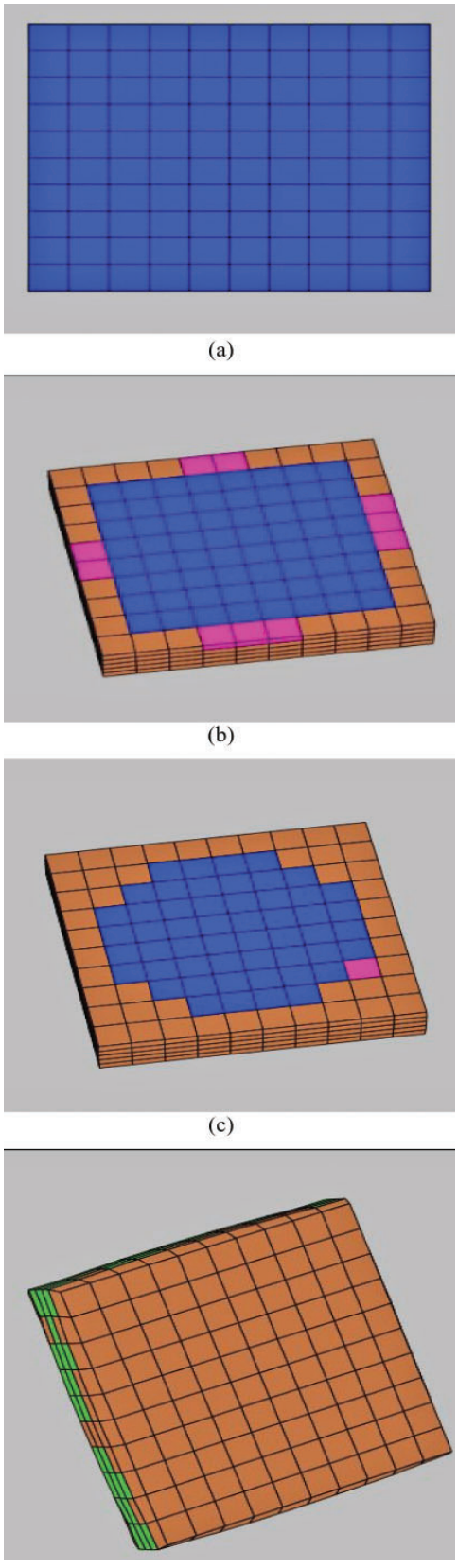

(a)

(b)

(c)

(d)

Fig.7 (a) to (d) showing gradual failure of coal pillar which starts from outer edge to inner core in the numerical model

3.0 Post failure stiffness

The concept of the stress-strain curve was given by Fairhurst and Cook (1966) to explain the behaviour of rock mass under stress conditions and perform laboratory tests to determine its strength. It was continued to estimate the post failure characteristics like magnitude of peak strength and slope of the post-failure for different width and height ratio by using servo-controlled uniaxial testing machine (Bieniawski, 1969; Bieniawski and Vogler, 1970; Wagner, 1974; Das, 1986; Zipf, 1999). However, measurement of the stress-strain behaviour of the pillars using laboratory tests is very difficult.

Post-failure stiffness is the tangent of the sloping curve of the stress-strain curve of the pillar as shown in Fig.1. The post-failure stiffness may depend on the temperature, confining pressure and loading rate (Zipf, 1999).

The study carried out by Singh (1986) shows that for Indian coalfield conditions, the post-failure characteristic starts regaining strength after initial fall showing elastic-plastic behaviour for the w/h ratio of 4-6, for w/h ratio 9-12 the post-failure slope is positive showing high strength with strain hardening behaviour and at less than 4-6, the residual strength becomes zero due to small pillars showing strain softening behaviour. A realistic estimation of the post-failure characteristic of wider pillars (w/h > 4-6) becomes rather difficult (Das, 1989; Zipf, 1999). However Zipf (1999) have reported that post-failure strength increases with w/h; at a ratio of 8, it is zero and beyond 8 is positive which is little unlike from the Das (1989).

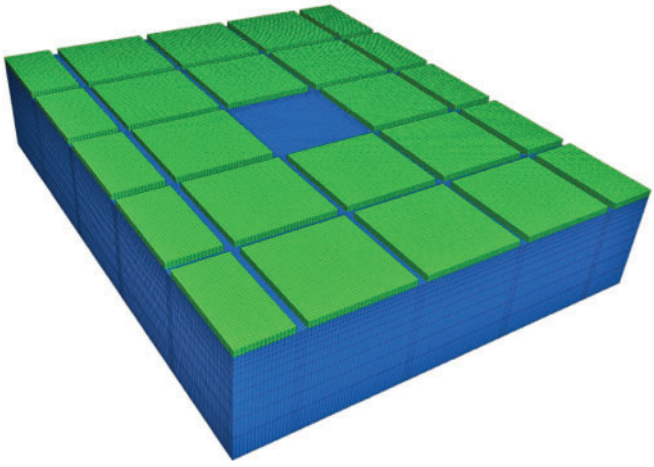

Fig.8 Numerical model of the developed seam where the middle pillar is removed

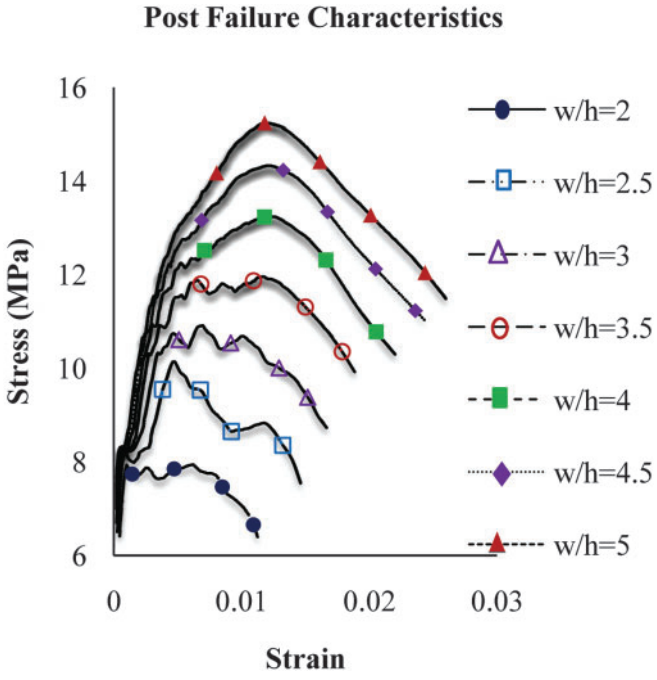

Fig.9 Post-failure stress-strain curve for 300m depth of cover

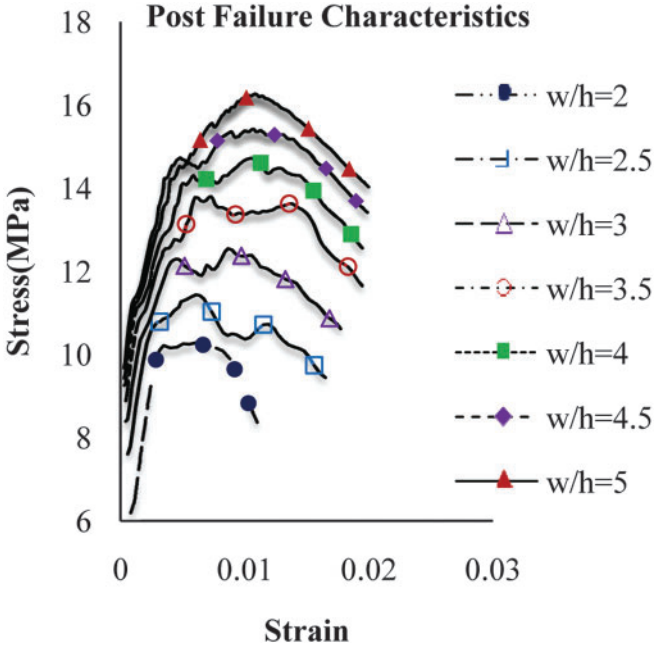

Fig.10 Post-failure stress-strain curve for 483m depth of cover

TABLE 4: TABULATION OF LOCAL MINE STIFFNESS AND POST FAILURE STIFFNESS

Depth of cover (m)	Average stress (MPa)	Average convergence with pillar (mm)	Average convergence without pillar (mm)	Local mine stiffness (MPa)	Post failure stiffness (MPa)
300	8.836	3.237	100.29	274.95	250
483	14.3555	6.596	285.49	155.45	200

Many other authors have done studies on post failure characteristic with respect to width and height using laboratory specimens like Wagner (1974), Bieniawski and Vogler (1970) and Chase et al. (1995).

A insight to use alternative approach to determine the average stress-strain and post failure stiffness of a pillar using numerical modelling (FLAC3D) started early of 1990 (Iannacchione, 1990; Zipf, 1997; Yavuz, 1999; Murli Mohan et al., 2001; Mandal, 2009; Das et al., 2014) and became a major realistic practice today.

Using the properties as listed in Tables 1 and 2, numerical models were simulated in FLAC3D with different width and height ratio ranging from 2 to 5. The in-situ stresses are used as per Table 3. The models were run till it reached equilibrium and the previously estimated strain softening parameters were used here as Mohr-Coulomb strain softening parameters. A FISH file is used to determine the average stress and average strain and plotted using the history function in the FLAC3D. The results were imported to excel and the graphs of different width to height ratios of post failure characteristicsare plotted as shown in Figs.9 and 10. The steepest part of the post-failure characteristic is the post failure stiffness.

4.0 Result and discussions

The local mine stiffness for the above-mentioned conditions are determined as per Eq. 12 and the results are tabulated in Table 4. The local mine stiffness is plotted against the post failure characteristics as shown in Figs.11 (a to g) and 12 (a to g).

At w/h ratio 2-5, the local mine stiffness is lesser than the post failure stiffness in all the graphs in Fig.11 (a to g). Hence, it can be stated, the failure in this condition would be stable (i.e., not abrupt and violent) and there is no chance of coal bump at a 300m depth of cover as per the geo-mining parameters used in the model.

At a 483m depth of cover of Digwadih colliery, the local mine stiffness obtained from the numerical modelling is almost near to the post failure stiffness as shown in Fig.12 (a to g). It can be stated that there is a chance of coal bump in the mine. As per the field observation stated earlier, the mines at 483m depth should be near to the burst-proneness category instead of burst-prone mine, but little over estimated may be due to the assumption of a number of physico-mechanical properties and in-situ stresses in the numerical models.

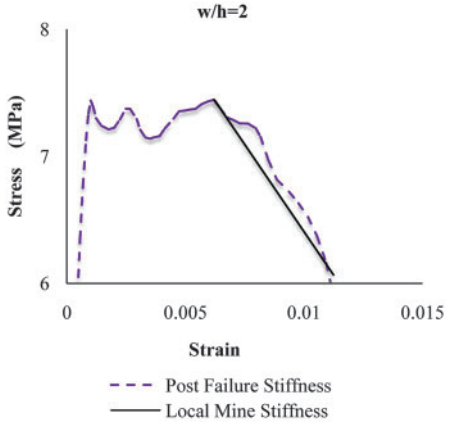

Fig.11(a) Stable or unstable failure for w/h = 2 with depth of seam 300m

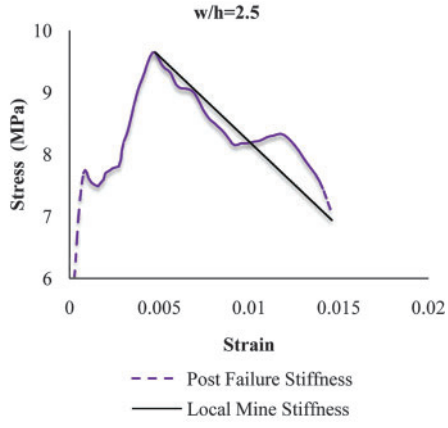

Fig.11(b) Stable or unstable failure for w/h = 2 with depth of seam 300m

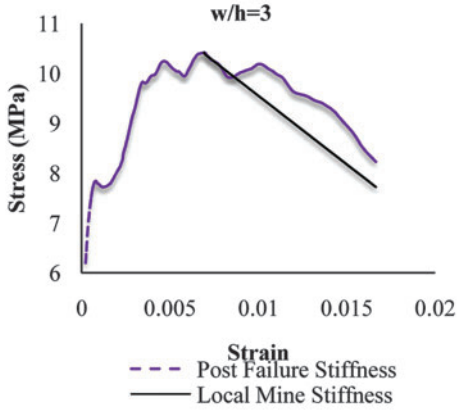

Fig.11(c) Stable or unstable failure for w/h = 3 with depth of seam 300m

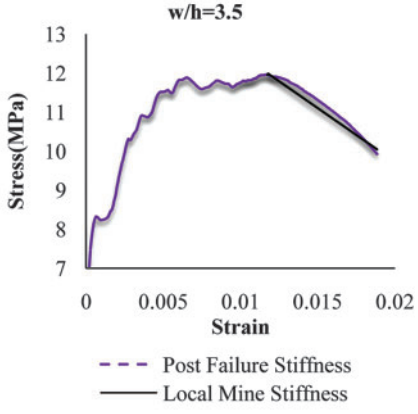

Fig.11(d) Stable or unstable failure for w/h = 3.5with depth of seam 300m

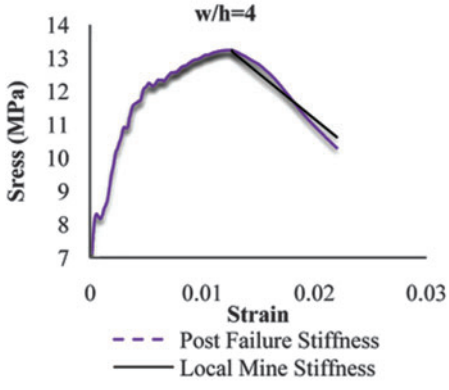

Fig.11(e) Stable or unstable failure for w/h = 4 with depth of seam 300m

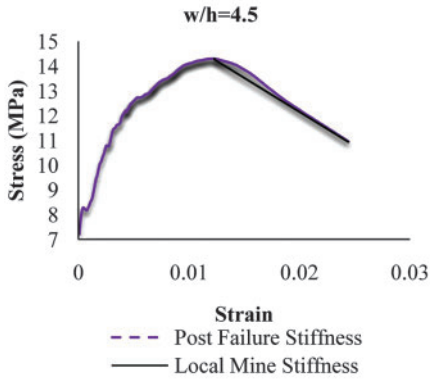

Fig.11(f) Stable or unstable failure for w/h = 4.5with depth of seam 300m

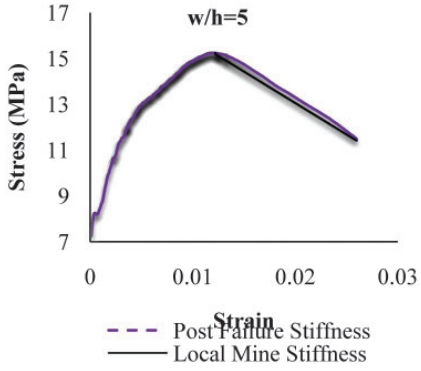

Fig.11(g) Stable or unstable failure for w/h=5 with depth of seam 30

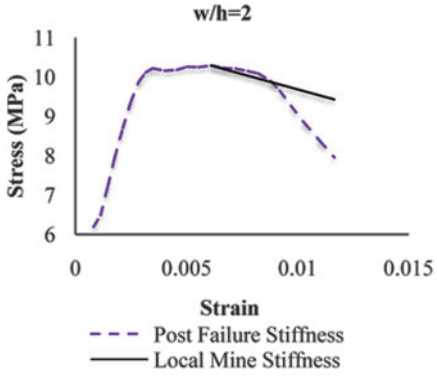

Fig.12(a) Stable or unstable failure for w/h=2 with depth of seam 483m

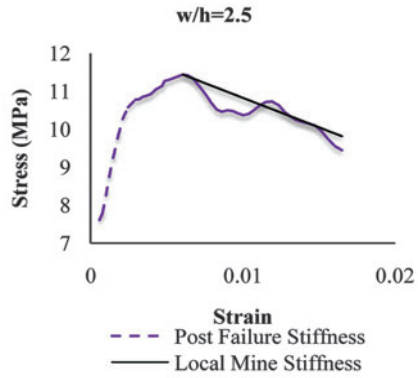

Fig.12(b) Stable or unstable failure for w/h=2.5 with depth of seam 483m

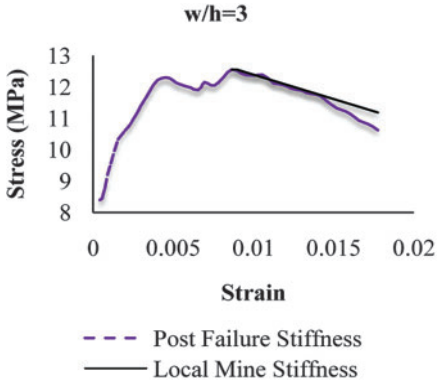

Fig.12(c) Stable or unstable failure for w/h=3 with depth of seam 483m

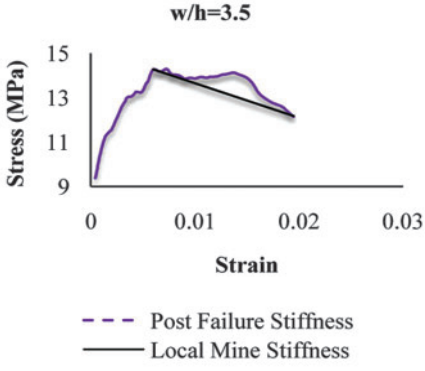

Fig.12(d) Stable or unstable failure for w/h=3.5 with depth of seam 483m

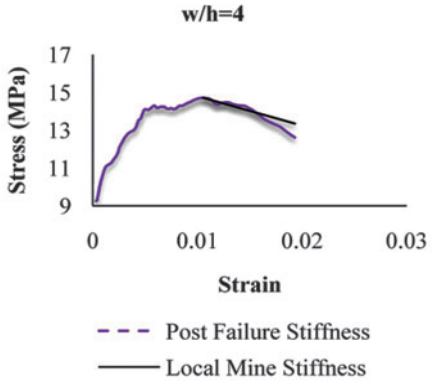

Fig.12(e) Stable or unstable failure for w/h=4 with depth of seam 483m

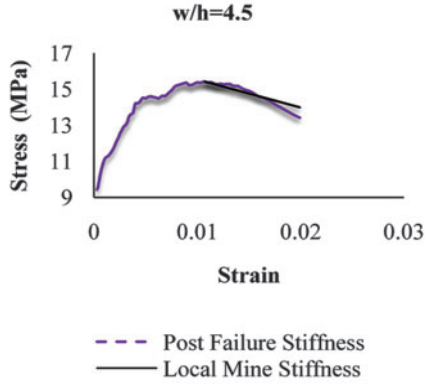

Fig.12(f) Stable or unstable failure for w/h=4.5 with depth of seam 483m

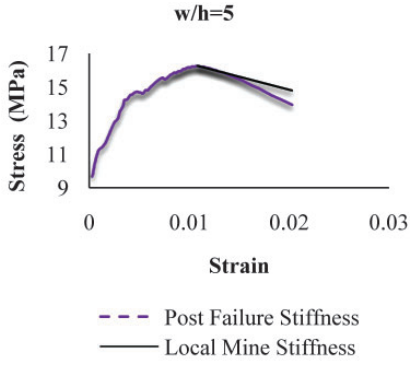

Fig.12(g) Stable or unstable failure for w/h=5 with depth of seam 483m

5.0 Conclusion

Uncontrolled failures progress very rapidly ahead of the development or during depillaring operation in a deep underground coal mining resulting in bump, which is very hazardous and violent in nature. If it is possible to identify the burst-proneness before the commencement of the mining operation, a suitable mining method and compatible support system can be suggested ahead of the working then major strata control problems can be avoided for the efficient extraction of coal with better production, productivity and safety. In this study, an effort has been made to identify burst-proneness of a mine by determination of local mine stiffness and post-failure characteristics of the mine through numerical modelling.

The conventional method of determining the post-failure characteristic is a tedious, expensive and time-consuming process. With the advent of numerical modelling techniques, it can be determined with ease. Using FLAC3D, the local mine stiffness is determined and compared to post-failure stiffness of the mine as shown in Figs.11 (a to g) and 12 (a to g) in this study. The obtained local mine stiffness for the 300 and 483m depth of cover are 274.95 and 155.45 MPa respectively as shown in Table 4. The postfailure stiffness is obtained from the numerical modelling which is 250 MPa and 200 MPa for 300m and 483m depths of cover respectively. At a 300m depth of cover, the local mine stiffness is greater than the post failure stiffness meeting the Salamon's criterion, where the pillar would fail in a stable manner and there is no chance of coal bump in

the mine as per the results of the numerical modelling. As described earlier, if the local mine stiffness is near or lesser than the post failure stiffness then the pillar may fail in a violent and unstable manner. In the case of working of Digwadih colliery at a 483m depth of cover, as per the numerical modelling, there is a chance of coal bump and field observation also supported the numerical modelling results. The numerical modelling results so obtained little over estimated the burst-proneness may be due to the assumption of a number of non-available parameters including some physico-mechanical properties and in-situ stresses. But, it can be concluded that if all the required data are available then the burst-proneness of a mine can be reasonably predicted in advance using numerical modelling.

6.0 Acknowledgements

The authors are obliged to the Directors, CSIR-Central Institute of Mining and Fuel Research, Dhanbad and Indian Institute of Technology (ISM), Dhanbad for their kind help and support for the study. Thanks are due to the management of the Digwadih colliery, Tata Steel for their valuable cooperation and support during the field observations. The views expressed in this paper are that of the authors and not necessarily of the organisation they belong to.

References

1. Anon1 (2017): "http://royalmining.blogspot.in/2015/10/which-is-deepest-mine-in-india.html" last accessed on August 10, 2017.
2. Bieniawski, Z. T. (1969): "Deformation Behavior of Fractured Rock under Multi-Axial Compression." Proceedings of the International Conference on Structures and Solid Mechanics Engineering Materials, Southampton, pp. 589-598.
3. Bieniawski, Z. T. and Vogler, U. V. (1970): "Load-Deformation Behavior of Coal after Failure." Proceedings of the Second ISRM Congress on Rock Mechanics, ISRM (Belgrade, Yugoslavia), 1, pp. 2-12.
4. Brauner, G. (1994): "Rockbursts in Coal Mines and Their Control." DMT, Essen, Germany, Balkema, 144p.
5. Chase, F. E., Mark, C. and Heasley, K. A. (2002): "Deep Cover Pillar Extraction in the U.S.A." Proceedings of the 21st International Conference on Ground Control in Mining, Morgantown, WV, USA, 68, pp. 132-150.
6. Chase, F. E., Zipf, R. K. and Mark, C. (1995): "The Massive Collapse of Coal Pillars - Case Histories from the United States." *International Journal of Rock Mechanics and Mining Sciences and Geomechanics Abstracts*, 8(32), p. 396A.
7. CMPDI (2015): "www.cmpdi.co.in/coal" accessed on 06/06/2017.
8. CMRI Report (1994): "A Study of Bump Proneness of Indian Coal Seams and Measures to Alleviate the Bump Hazard." *Coal S&T Grand-in-Aid Project Report*, Central Mining Research Institute, Dhanbad, 124p.
9. CMRI Report (2002): "In-situ Stress Measurement in Underground Coalmines and its Application to Stability Analysis." *Ann. Sci. Tech. Rep.*, 88p.
10. Crouch, S. L. and Fairhurst, C. (1974): "Mechanics of Coal Mine Bumps." *Trans. SME of AIME*, 256, pp. 317-322.
11. Das, A. J., Mandal, P. K., Kumbhakar, D. and Mishra, P. K. (2014): "Effect of Rib Pillars at Higher Depth of Working: A Numerical Modelling Based Study." *Mining Engineers' Journal*, 16 (2), pp. 23-30.
12. Das, M. N. (1986): "Influence of Width/Height Ratio on Postfailure Behavior of Coal." *International Journal of Mining and Geological Engineering*, 4(1), pp.79-87.
13. Dou, L. M. and He, X. Q. (2001): "Prevention theory and technology of rock burst." Xuzhou: China University of Mining and Technology Press, 2001, 270p.
14. Fairhurst, C. and Cook, N. G. W. (1966): "The Phenomenon of Rock Splitting to the Direction of Maximum Compression in the Neighborhood of a Surface." Proceedings of the First Congress of International Society of Rock Mechanics, Lisbon, 1, pp. 687-692.
15. Garvey, R. J. (2013): "A Study of Unstable Rock Failures using Finite Difference and Discrete Element Methods." PhD Thesis, Department of (Mining and Earth Systems Engineering Colorado School of Mines, 224p.
16. Ghose, A. K. (1988): "Bumps and Rockbursts in Indian Coal Mines- An Overview." Proceedings of the Fifth Planetary Scientific Session of Working Group on Rock bursts of International Bureau of Strata Mechanics, Rockbursts Global Experience, Organized by Institution of Engineers, Hyderabad, India, 2nd-3rd February, pp 123-129.
17. Haramy, K. Y. and McDonnell, J. P. (1988): "Causes and Control of Coal Mine Bumps." *US Bureau of Mines, Report of Investigations 9225*, 34p.
18. Iannacchione, A. T. (1990): "Behavior of a Coal Pillar Prone to Burst in the Southern Appalachian Basin of the United States." Proceedings of Rockbursts and Seismicity in Mines, Balkema, pp. 295-300.
19. Iannacchione, A. T. and Stephen, C. T. (2008): "Coal Mine Burst Prevention Controls." Proceedings of 27th International Conference on Ground Control in Mining, Morgantown, 29th-31st July, pp. 20-28.
20. Itasca (2012): "FLAC3D (Fast Lagrangian Analysis of Continua in 3 Dimensions)." Itasca Consulting Group Inc., Version 5.0, Minneapolis, Minnesota, 55401, USA.
21. Jiang, Y., Zhao, Y., Wang, H. and Zhu, J. (2017): "A Review of Mechanism and Prevention Technologies of Coal Bumps in China." *Journal of Rock Mechanics and Geotechnical Engineering*, 9 (1), pp. 180-194.
22. Justine, C. and Jan, N. (2016): "Coalburst Causes and

Mechanisms." Proceedings of the 16th Coal Operators' Conference, Mining Engineering, University of Wollongong, 10-12 February, pp. 310-320.

23. Khair, A. W. (1985): "An Analysis of Coal Bump Liability in a Bump Prone Mine." *International Journal of Mining Engineering*, 3 (4), pp. 243-259.
24. Kidybinski, A. (1981): "Bursting Liability Indices of Coal." *International Journal of Rock Mechanics, Mining Sciences and Geomechanics Abstracts*, 18(4), pp. 295-304.
25. Mandal, P. K. (2009): "Development of a Methodology for Underground Extraction of Contiguous and Thick Contiguous Coal Seams/Sections under Weak and Laminated Parting." Ph.D Thesis, Department of Mining Engineering, Bengal Engineering and Science University, Shibpur, Howrah, 313p.
26. Mark, C. and Chase, F. E. (1997): "Analysis of Retreat Mining Pillar Stability (ARMPS)," Proceedings of the New Technology for Ground Control in Retreat Mining, NIOSH, IC9446, pp. 17-34.
27. Murali Mohan, G., Sheorey, P. R. and Kushwaha, A. (2001): "Numerical Estimation of Pillar Strength in Coal Mines." *International Journal of Rock Mechanics and Mining Sciences*, 38(8), pp. 1185-1192.
28. Ozbay, U. (2015): "Numerical Modelling Methodologies For Assessing Burst Potential In Coal Mines." 1st Solicitation for Single Investigator Research Grants, *Final Technical Report, Alpha Foundation for the Improvement of Mine Safety And Health. Colorado School of Mines*, 69p.
29. Pan, Y. S., Li, Z. H. and Zhang, M.T. (2003): "Distribution, Type, Mechanism, and Prevention of Rock Burst in China." *Chinese Journal of Rock Mechanics and Engineering*, 22 (11), pp. 1844-1851.
30. Pang, X., Jiang, Y., Zhao, Y. and Zhu, J. (2011): "Study on Risk Analysis and Control Technology of Coal Bump." Proceedings of Environmental Sciences, 12, pp. 832-836.
31. Petr, K., Kamil, S., Lubomir, S., Singh, R. and Sinha, A. (2010): "Practices to Control Rock Burst in Deep Coal Mines of Upper Silesian Coal Basin and their Applicability for Dishergarh Seam of Raniganj Coalfield." Proceedings of International Symposium - 6th Asian Rock Mechanics Symposium, 23-27 October, New Delhi, India, 16p.
32. Rice, G. S. (1934): "Bumps in Coal Mines-Theories of causes and Suggested means of Prevention or of Minimizing." *Trans AIME*, pp. 3-23.
33. Salamon, M. D. G. (1970): "Stability, Instability, and Design of Pillar Workings." *International Journal of Rock Mechanics, Mining Sciences and Geomechanics Abstract*, 7(6), pp. 613-631.
34. Salamon, M. G. D. (1992): "Strength and stability of coal pillars." *Workshop on Coal Pillar Mechanics and Design*, pp. 94-121.
35. Sheorey, P. R. (1994): "A Theory for In-situ Stresses in Isotropic and Transversely Isotropic Rock." *International Journal of Rock Mechanics, Mining Sciences and Geomechanics Abstract*, 31(1), pp. 23-34.
36. Sheorey, P. R. (1997a): "Empirical Rock Failure Criteria." CRC press, Balkema, Rotterdam, 1997a, 176p.
37. Sheorey, P. R. and Singh, B. (1988): "Case Studies of Depillaring Under Special Strata and Mining Conditions." Proceedings of 7th International Conference on Ground Control in Mining, Morgantown, pp. 351-357.
38. Sheorey, P. R., Barat, D., Prasad, R. K. and Das, M. N. (1997b): "Identification of Burst-Prone Coals and a Preliminary Proposal for Bord and Pillar Mining in a Deep Coal Seam." Proceedings of 27th International Conference Safety in Mines Research Institutes, New Delhi. Oxford and IBH, pp. 825-832.
39. Sheorey, P. R., Murali Mohan, G. and Sinha, A. (2001): "Influence of Elastic Constants on the Horizontal In-situ Stresses." *International Journal of Rock Mechanics, Mining Sciences and Geomechanics*, 38, pp. 1211-1216.
40. Wagner, H. (1974): "Determination of the Complete Load-Deformation Characteristics of Coal Pillars." Proceedings of the Third Congress of the International Society for Rock Mechanics, Denver, pp. 1076-1081.
41. Wen, Z., Wang, X., Tan, Y., Zhang, H., Huang, W. and Li, Q. (2016): "A Study of Rockburst Hazard Evaluation Method in Coal Mine." Shock and Vibration, Article ID 8740868, Hindawi Publishing Corporation, 9p.
42. Yavuz, H. (1999): "Numerical and Physical Modelling of Pillar Protected Mine Roadways." PhD. Thesis, Leeds University, 252p.
43. Yavuz, H. (2001): "Yielding Pillar Concept and its Design." Proceedings of 17th International Mining Congress and Exhibition, Turkey- MCET, pp. 397-404.
44. Yixin, Z., Yaodong, J., Jie, Z., Zhi-ping, W. and Wen-fei, Z. (2009): "Investigation on the Precursors of Bump Prone Coal Failure." The 6th International Conference on Mining Science and Technology, Procedia Earth, and Planetary Science, 1(1), pp. 530-535.
45. Zhang, C., Canbulat, I., Tahmasebinia, F. and Hebblewhite, B. (2017): "Assessment of Energy Release Mechanisms Contributing to Coal Burst." *International Journal of Mining Science and Technology*, 27(1), pp. 43-47.
46. Zhao, X. Y. and Jiang, D. Y. (2009): "Investigation on the Mechanism of Coal bumps and Relating Microscopic Events." Proceedings of the 3rd CANUS Rock Mechanics Symposium, Toronto, May, Paper 4158, 10p.
47. Zipf, R. K. (1999): "Using a Post Failure Stability Criterion in Pillar Design." Proceedings of the Second International Workshop on Coal Pillar Mechanics and Design, Pittsburgh, PA, June, pp. 178-190.